THE JOURNAL OF PHYSICAL CHEMISTRY C

Pacific Northwest NATIONAL LABORATORY
Proudly Operated by Battelle Since 1965

C: Physical Processes in Nanomaterials and Nanostructures

Evolution of Ion–Ion Interactions and Structures in Smectic Ionic Liquid Crystals

Seo Kyung Park, Kee Sung Han, Jin Hong Lee, Vijayakumar Murugesan, Seung Hyun Lee, Chong Min Koo, Je Seung Lee, and Karl T. Mueller

J. Phys. Chem. C, **Just Accepted Manuscript** • DOI: 10.1021/acs.jpcc.9b04056 • Publication Date (Web): 26 Jul 2019

Evolution of Ion–Ion Interactions and Structures in Smectic Ionic Liquid Crystals

Seo Kyung Park,[†,⊤] Kee Sung Han,[‡,⊤] Jin Hong Lee,[∥] Vijayakumar Murugesan,[‡] Seung Hyun Lee,[†] Chong Min Koo,[§] Je Seung Lee,*[,†] and Karl T. Mueller*[,‡]

[†]Department of Chemistry and Research Institute of Basic Sciences, Kyung Hee University, 26 Kyungheedae-ro, Dongdaemun-gu, Seoul 02447, Republic of Korea

[‡]Physical and Computational Sciences Directorate, Pacific Northwest National Laboratory, Richland, WA 99352, United States

[∥]Department of Organic Material Science and Engineering, Pusan National University, Busan 46241, Republic of Korea

[§]Materials Architecturing Research Center, Korea Institute of Science and Technology, Seoul 02792, Republic of Korea

ABSTRACT: Mixture of ionic liquid, 1,3-dimethylimidazolium 2-methoxy(2-ethoxy(2-ethoxy(2-ethoxy)))ethylphosphite ([DMIm][MPEGP]), and lithium bis(trifluoromethanesulfonyl)imide (LiTFSI), which forms an ionic liquid crystal with a superior ionic conductivity, evolves a smectic structure through ion–ion interactions as a function of LiTFSI concentration. Nuclear magnetic resonance (NMR) spectroscopy and pulsed field gradient (PFG) NMR examinations showed that the morphology of the structures and the strength of ion–ion interactions are closely related to the ratio of Li^+/$[MPEGP]^-$. The results revealed structures composed of Li^+ : $[MPEGP]^-$: $TFSI^-$ (≈ 3 : 4 : 1) mainly by the Coulombic interactions between Li^+ cations and phosphite head groups in $[MPEGP]^-$ anions. NMR diffraction on PFG-echo profiles revealed a cluster size of ~ 2 μm, inversely proportional to the number of mobile $[MPEGP]^-$ anions, and an ion diffusion on the cluster surfaces that is 1000 times faster than that in the bulk liquid. These observations suggest that the superior ionic conductivity in the mixture is mainly due to the fast ion transport on the cluster surfaces of smectic ionic liquid crystals. The variations of diffusion ratios between mobile Li^+, $TFSI^-$, $[DMIm]^+$, and $[MPEGP]^-$ ions indicate that these mobile ions remaining in the voids of structures preserve the bulk ionic liquid properties.

INTRODUCTION

Room temperature ionic liquids (RTILs) are well known for their unique properties such as ignorable volatility, non-flammability, superior chemical and thermal stability, wide electrochemical window, and high ionic conductivity.[1,2] These properties can be controlled through modification of cation/anion structures or by pore confinement, resulting in host-guest interactions, or in both ways.[3,4] These designable properties have been found useful for various potential applications including as green solvents, electrolytes for electrochemical devices such as batteries, fuel cells and supercapacitors, biosensors, and drug release systems.[1,5,6] In cases where RTILs act as the solvents for electrolytes in electrochemical devices, they should have large active ion transference numbers with minimum degradation during repetitive charge/discharge processes. To obtain the required properties, ILs can be easily modified.[7-10]

Recently, we have reported the facilitated ion transport phenomena in mixtures of ionic liquid (1,3-dimethylimidazolium 2-methoxy(2-ethoxy(2-ethoxy(2-ethoxy)))ethylphosphite, [DMIm][MPEGP]) and lithium bis(trifluoromethanesulfonyl)imide (LiTFSI).[11] In those mixtures, the diffusion of ions on the surfaces of cluster is faster by three orders of magnitude compared to the bulk system. This is quite different behavior than that of the Li^+ cation diffusion in polymer electrolytes containing LiTFSI, which showed similar ion transport properties between the ions in the bulk and on the cluster surfaces.[12-14] In addition, these mixtures form a smectic ionic liquid crystal structure with a layer spacing of 4.36 nm with superior ionic conductivity (σ) over neat [DMIm][MPEGP] when the molar ratio of LiTFSI/ [DMIm][MPEGP] ≥ 0.4.

Our studies also suggested that the structure formation is due to the Coulombic interactions between dissolved Li^+ cations and oxygen atoms in the center of $[MPEGP]^-$ anions. This structure formation mechanism is quite different from that of the polyethylene oxide-based polymer electrolytes, which form additional structures from the interactions of Li^+ cations with the oxygen atoms on the polyethylene oxide chains,[13,15] by reducing self-aggregation in the pyrrolidinium-based IL[16] and diminishing Li^+–solvent interactions in the $LiPF_6$ dissolved organic solvent.[17] Moreover, these mixtures showed minima on the pulsed-field-gradient (PFG) echo profiles in the PFG-NMR examination, which is referred to as 'NMR diffraction' due to the structure formations.[13,14]

In this work, the evolution of structures and ion–ion/ion–solvent interactions in mixtures of [DMIm][MPEGP] and LiTFSI were systematically studied using NMR spectroscopic techniques. The samples were prepared by mixing [DMIm][MPEGP] and LiTFSI with variation of relative concentrations ($0 \le x \le 3$, where x is the molar ratio of LiTFSI/[DMIm][MPEGP]). The NMR diffraction behavior in PFG-NMR examination of the mixtures and their resulting macroscopic properties, such as the ionic conductivity (σ), were also investigated.

Scheme 1. Chemical structure of [DMIm][MPEGP]. The numerals label the proton resonances.

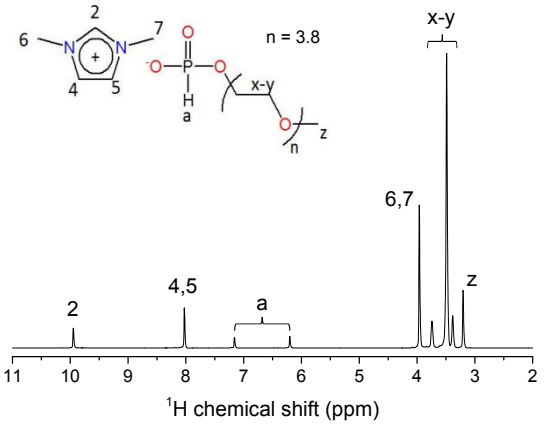

EXPERIMENTAL

Samples Preparation. The ionic mixtures were prepared according to a previously reported procedure.[11] In a typical experiment, the proper amount of LiTFSI was dissolved in a [DMIm][MPEGP] mixture. The lithium salt contents were varied between x = 0 and x = 3.0, where x is the molar ratio of components (moles of LiTFSI/moles of [DMIm][MPEGP]). The mixtures were placed into NMR tubes and dried at 100 °C for 48 h under vacuum and then sealed prior to running the NMR experiments.

Impedance Analysis. The ionic conductivity of each of the ionic mixtures was measured using a complex impedance analyzer (Bio-Logics, VMP3) over frequencies ranging from 100 MHz to 1 MHz at an AC amplitude of 10 mV. The real value of the impedance at the minimum of the imaginary part was taken as the resistance of ionic mixtures. The ionic conductivities were calculated as $\sigma = \frac{d}{A \times R}$, where R is the resistance, d is the sample thickness, and A is the electrode surface area.

SAXS Examinations. Synchrotron SAXS experiments were carried out on the 4C1 SAXS beamline at the Pohang Light Source, Republic of Korea. The wavelength of the monochromatic X-ray beams was 0.6754 Å and the distance between sample and detector was 2 meters.

NMR and PFG-NMR Examinations. For the range of samples (x = 0-3, where x is the molar ratio of LiTFSI to [DMIm][MPEGP] (see Figure S1 in Supporting Information, SI)), the ^{7}Li, ^{19}F, ^{1}H, and ^{31}P NMR spectra were obtained at 293 K. Diffusion coefficients (D) of Li^+, $TFSI^-$, $[DMIm]^+$, and $[MPEGP]^-$ ions, denoted as D_{Li}, D_{TFSI}, $D_{[DMIm]}$, and $D_{[MPEGP]}$, respectively, were determined within the range of 293–353 K. All NMR spectra were obtained using a single pulse excitation with 90° pulse lengths of 12, 5.5, and 7 μs for ^{7}Li, ^{1}H, and ^{19}F, respectively. The ^{7}Li, ^{19}F, ^{1}H PFG-NMR examinations were performed with a bipolar gradient stimulated echo (Dbppste, a vender supplied pulse sequence in VNMRJ, Agilent, USA). The diffusion coefficients of $[DMIm]^+$ cation and $[MPEGP]^-$ anion were simultaneously measured using ^{1}H PFG-NMR from the ^{1}H resonances of $[DMIm]^+$ cation, H(2), and the polyether chains of $[MPEGP]^-$, H(a), respectively (Scheme 1). The number of mobile ions for Li^+, $[DMIm]^+$, $[MPEGP]^-$, and $TFSI^-$ ions were estimated from the intensities of ^{7}Li, ^{1}H, ^{31}P, and ^{19}F peaks, respectively, as a function of x because of the invisibility of immobile ions in the liquid-state NMR spectra.[18] All NMR examinations were performed on a 600 MHz NMR spectrometer (Agilent Technology, USA) equipped with a 5 mm z-gradient probe (Doty Scientific, USA) with a maximum gradient strength of ~31 T m^{-1}. The PFG-echo profiles were recorded as a function of gradient strength (g) and fitted with the Stejskal-Tanner equation:[19]

$$S(g) = S(0)\, exp[-D(\gamma g \delta)^2(\Delta - \delta/3)] \quad (1)$$

where $S(g)$ and $S(0)$ are the echo heights at the gradient strengths of g and 0, D is the diffusion coefficient, γ is the gyromagnetic ratios of ^{7}Li, ^{1}H, or ^{19}F, Δ is the diffusion delay, which is the time interval between the two pairs of bipolar pulse gradients, and δ is the gradient length.[20] The gradient strength was varied with 15 equal steps and the maximum gradient strengths (in the range of 0.4 - 25 T m^{-1}) were chosen accordingly to observe a full decay of echo. The gradient durations δ were 2 - 4 ms. The diffusion delay Δ varied from 20 to 40 ms for ^{7}Li and ^{1}H PFG-NMR and was constant at 4 ms for all ^{19}F PFG-NMR. The apparent diffusion coefficients obtained preliminary as a function of Δ indicated that the diffusion coefficients measured with the above Δ values all represent motion in the steady-state diffusion regime.[4]

RESULTS AND DISCUSSION

Origin of Structures. Phase structures of the ionic mixtures prepared by mixing the anion functionalized ionic liquid of [DMIm][MPEGP] with lithium salt were investigated using photography (Figure S1) and SAXS (Figure S3) techniques. The observed structures have been illustrated in our previous report (Figure S4).[11] In SAXS examinations, completely featureless patterns in the range of $0 \le x \le 0.3$ were observed, indicating that the structural order does not result from the self-assembly of the neat ionic liquid. The prepared mixtures were transparent liquids in this range of $0 \le x \le 0.3$ (Figure S1). Remarkably, when the lithium salt content was increased ($0.4 \le x \le 1$), the ionic mixtures became opaque and gave rise to a smectic liquid crystal phase with layer-by-layer positional order in the gel state. In this range of molar ratio, the mixture behaved like a cloudy gel, not a liquid. Upon increasing the lithium content, the structural order reached a maximum at x = 0.8 and was steadily reduced when the content of lithium salt was increased. Meanwhile, in systems with excess lithium salt content ($1 \le x$), the mesostructures converted into weakly segregated structures and behaved like highly viscous turbid liquids. To evaluate the structure evolution in the mixtures of

LiTFSI and [DMIm][MPEGP], the variations of the number of mobile ions were monitored as a function of x.

Based on the similar decrement of ^{31}P peak intensity and H(a)/H(2) (≈ number of mobile [MPEGP]$^-$/number of mobile [DMIm]$^+$ ratio in ^{1}H NMR spectra (Figure S2),[11] it is assumed that [DMIm]$^+$ cations do not directly contribute to the structure formation. If there was a contribution of [DMIm]$^+$ cations to the structure formation the ratio H(a)/H(2) should be larger than the ^{31}P peak intensity owing to the loss of H(2) intensity due to the existence of immobile [DMIm]$^+$ cations. Then, as shown in Figure 1a, the numbers of mobile [DMIm]$^+$ cations were almost the same for all samples. This observation strongly suggests that the head group of [MPEGP]$^-$ anions is directly related to the structure formation. Both the number of Li$^+$ cations and [MPEGP]$^-$ anions changed abruptly at x = 0.3 and 0.8 with a minimum at x = 0.8. This result clearly indicates that the structure is mainly composed of Li$^+$ cations and [MPEGP]$^-$ anions and almost all available Li$^+$ cations and [MPEGP]$^-$ anions are participating in the structure formation at x = 0.8. The samples with x = 0.5 and 0.6 showed that all Li$^+$ cations participate in the structure formation process; however, mobile [MPEGP]$^-$ anions still exist. These observations strongly suggest that the clusters are composed of ions with a certain stoichiometry. The number of mobile TFSI$^-$ anions at x ≥ 0.4 (Figure 1a) slightly decreased, suggesting that certain amounts of TFSI$^-$ anions participate in the structure formation as well. As LiTFSI content in the mixture increased further from x = 0.8, the number of mobile Li$^+$ ions increased; here, however, [MPEGP]$^-$ anion remained the same. This behavior is probably due to the excess of LiTFSI after consuming available mobile [MPEGP]$^-$ anions. From the discontinuities at x = 0.3 and 0.8, we have assigned the mixtures to the three different morphological phases in our previous report: I) *localized* (short distance) *interaction* at 0 ≤ x ≤ 0.3, II) *global structure formation* at 0.3 < x ≤ 1, III) *LiTFSI excess* at 1 < x, which are in very good agreement with the morphological changes in the mixtures (Figure S1) and nanoscale information from the SAXS results (Figures S3).[11] Similar Li salt effects on morphological variation were observed in *N*-butyl-*N*-methyl-pyrrolidinium bis(trifluoromethanesulfonyl)imide, [BMP][TFSI], exhibiting crystallization at molar ratio of 0.377 for LiTFSI to [BMP][TFSI].[21] The above observations indicate that the structure with a specific stoichiometry forms mainly through the interaction between Li$^+$ cations and the head group of [MPEGP]$^-$ anions.

To elucidate the origin of the structure formation, the interaction between Li$^+$ cations and [MPEGP]$^-$ anions were studied through comparing ^{31}P NMR chemical shift (δ) and P-H coupling constant (J_{PH}) (Figure 2a), which are proportional to the electrostatic interaction between Li$^+$ cations and [MPEGP]$^-$ anions.[22] The multiple resonances of **a**, **b`**, and **b``** (Figure 2a) suggest that the ion distributions around [MPEGP]$^-$ anions became more heterogeneous at x ≥ 0.4. The ^{31}P NMR spectra showed that as LiTFSI concentration increased, the J_{PH} values gradually increased with a downfield shift of δ (Figure 3). This behavior is due to the enhancement of electrostatic interaction between Li$^+$ cations and [MPEGP]$^-$ anions.[22] In the range of 0 ≤ x ≤ 0.3, the peak **b`** gradually shifted downfield with increasing J_{PH} because the interactions between Li$^+$ and [MPEGP]$^-$ were restricted within a short distance range (Figure S1). However, in the samples of x = 0.5 and 0.6, two additional doublets (**a** and **b``**) were exhibited and the $\delta$($^{31}$P) and $J_{PH}$ of the peak **a** increased also. Meanwhile, $J_{PH}$ of the peak **b``** increased while its δ(^{31}P) shifted to more upfield than pure IL. This observation may be due to the varied solvation structure of Li$^+$ cation according to the numbers of mobile Li$^+$, TFSI$^-$ and [MPEGP]$^-$ ions.[22] To understand this behavior, DFT calculations were performed on Li$^+$ cation solvation clusters with varied numbers of TFSI$^-$ and [MPEGP]$^-$ anions (Figure S5). The J_{PH} values in all examined compositions increased by the addition of LiTFSI to pure [DMIm][MPEGP]. Although the Li$^+$ solvation shell with more [MPEGP]$^-$ than Li$^+$ and TFSI$^-$ exhibited downfield shifted δ(^{31}P), the compositions with ratios of Li$^+$: [MPEGP]$^-$: TFSI$^-$ = 1 : 1 : 1 and 1 : 1 : 3 showed upfield shifted δ(^{31}P) as observed from peak **b``**. Thus, it can be concluded that the peak **b``** is related to Li$^+$ cation solvation structures with a lack of mobile [MPEGP]$^-$ anions. It also could be suggested that the peak **a** was closely related to [MPEGP]$^-$ anions distributed in the vicinity of the smectic ionic liquid crystals surfaces because it appeared only after the formation of structures (x ≥ 0.5).

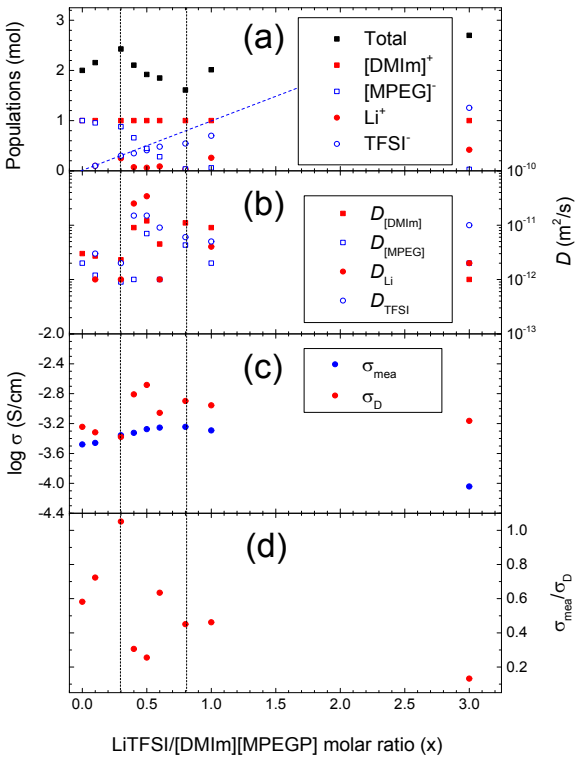

Figure 1. (a) Relative ion populations estimated from intensities of ^{1}H, ^{31}P, ^{7}Li, and ^{19}F NMR peaks, (b) diffusion coefficients of mobile ions, (c) ionic conductivity values measured using impedance spectroscopy (σ_{mea}) and diffusion

coefficients (σ_D), and (d) the degree of cation-anion dissociation (σ_{mea}/σ_D) in the mixtures of [DMIm][MPEG] and LiTFSI as a function of the LiTFSI content of x. All measurements were performed at 293 K.

The ^{31}P NMR spectrum of the x = 0.8 sample only showed a small peak **a** because of the strong interactions between Li^+ cations and $[MPEGP]^-$ anions. In addition, the ^{7}Li NMR spectrum of the x = 0.8 sample exhibited an additional broad component similar to the solid-state Li ion conductors and electrolytes[23,24] implying that the mobile Li^+ cations were also strongly bound to the clusters. Interestingly, the peak intensity of **a** slightly increased and the peak **b`** reappeared in the mixture with x = 1.0. This might be due to the presence of excess LiTFSI because the mobile $[MPEGP]^-$ and $TFSI^-$ anions could share Li^+ cations similar to x = 0.5 and 0.6 samples. For the x = 3 sample, both ^{7}Li and ^{31}P NMR peaks became broad mainly due to the lower mobility of ions due to the existing excess LiTFSI as well as the structural diversity. Sensitive variations in $\delta(^{31}P)$ and J_{PH} were also observed due to the changing composition of mobile species as a function of the addition of LiTFSI.

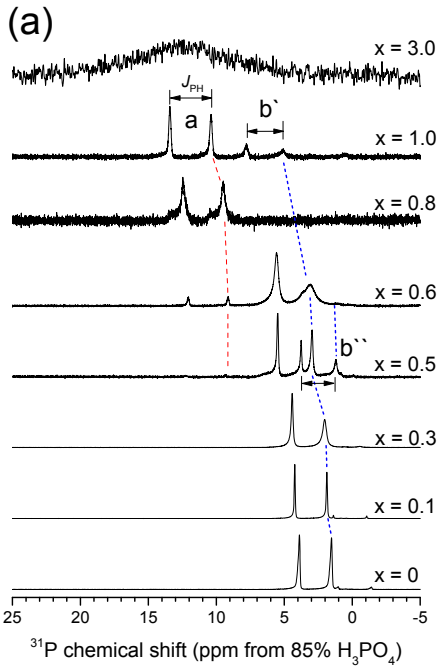

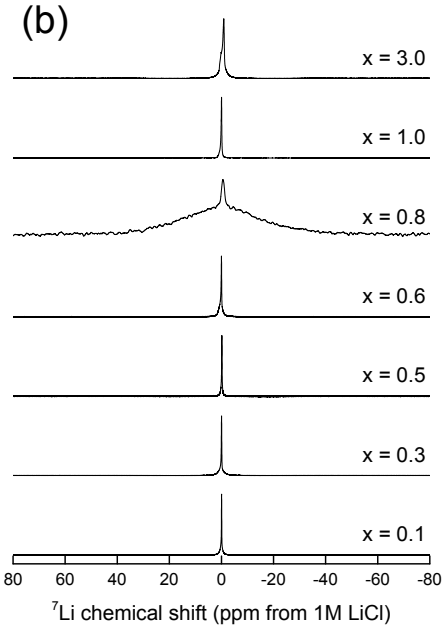

Figure 2. (a) ^{31}P and (b) ^{7}Li NMR spectra of [DMIm][MPEGP] mixed with LiTFSI obtained at 293 K as a function of LiTFSI content. The dashed lines guide the right peaks of each doublet.

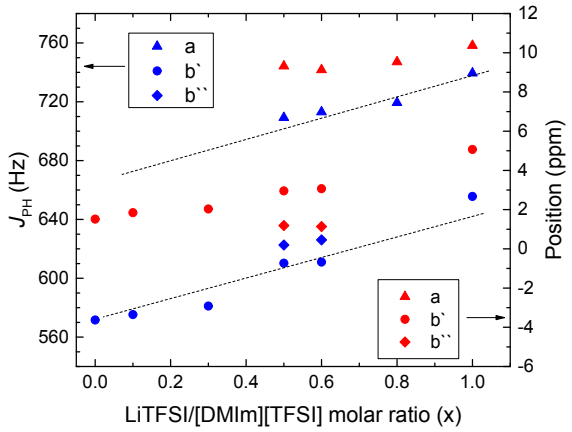

Figure 3. LiTFSI content dependence of J_{PH} and chemical shift of the left peaks for three doublets of **a** (triangles), **b`** (circles), and **b``** (diamonds). The lines are guides for the eye.

Diffusional Motion of Mobile Ions. Diffusion coefficients of each ions (D_{Li}, D_{TFSI}, $D_{[DMIm]}$, and $D_{[MPEGP]}$) for the mixtures were determined as a function of the amount of LiTFSI. However, it was not possible to measure the D_{Li} at x = 0.8 using ^{7}Li PFG-NMR due to short ^{7}Li relaxation times (T_1 and T_2) resulting from a strong interaction of Li^+ cation with the clusters. Therefore, it was assumed to be similar to D_{Li} in

solid-state Li electrolytes[23,24] based on the ^{7}Li NMR line shape. The D values obtained at 293 and 353 K, presented in Figures 1b and 4, respectively, varied complicatedly with LiTFSI content as a consequence of structure formation, ion–ion/ion–cluster interactions and the different number of mobile ions. Therefore, the diffusion ratio between the constituent ions also varied because the strength of interaction between ion–ion and ion–cluster changed by temperature and the composition of mobile ions.

As shown in Figure 1a and 1b, the ion diffusion coefficients are globally inversely proportional to the total number of mobile ions, except for the range of $0.4 \le x \le 1$, agreeing well with the previous report.[25] Noticeably, the diffusion coefficients obtained in the range of $0.4 \le x \le 1$ were 2 - 4 times faster than that of neat [DMIm][MPEGP] (x = 0) at 293 K as a consequence of structure formation. Similar enhancement of D and σ were observed from the polymer electrolytes doped with LiTFSI due to the improved flexibility of polymer chains.[26,27] Based on the Stokes-Einstein formula of $D = k_B T/6\pi\eta r_s$[28] (where k_B is Boltzmann constant, T is absolute temperature, η is solution viscosity, and r_s is the hydrodynamic radius of diffusing molecules), the strength of interactions of the observed ions to the other constituents was estimated. In the x = 0.1 sample, $D_{[DMIm]}$, D_{TFSI}, and $D_{[MPEGP]}$ were found similar to those obtained from neat ILs, [DMIm][TFSI] and [DMIm][MPEGP], indicating that small amounts of LiTFSI weakly affected the properties of the mixtures (Figure 4). Generally, the ions diffuse slower in the mixture than in the pure ILs due to the high viscosity attributed to increased ion-ion interactions. Usually, in mixtures of Li salt and an ionic liquid, D_{Li} has the smallest value among the constituents and decreases with the increase of Li salt content.[21,29,30] When LiTFSI content was increased in the LiTFSI/[DMIm][MPEGP] mixtures, the diffusion coefficients globally reduced from x = 0 to 0.3. Similarly, the ion diffusion in the LiTFSI/[BMP][TFSI] mixtures showed a gradual decrease of diffusion coefficient until the molar ratios of LiTFSI/[BMP][TFSI] reached x = 0.377, where crystallization occurred with a sudden ion conductivity loss.[21] However, examinations of LiTFSI/[DMIm][MPEGP] mixtures showed faster diffusion after gelation (at $x > 0.3$) at a lower temperature (293 K) and the diffusion was reduced again at $x \ge 0.8$.

Diffusion of Li^+, which was the slowest at $x \le 0.3$, became also fast after gelation at temperatures of 293 K (Figure 1b) and 353 K (Figure 4). These observations indicate that Li^+ ion diffusion is facilitated by the formation of structures. Although, the relative diffusion coefficients can be varied due to the different interactions between the constituent ions, the chain flexibility can also influence the diffusion of ions. For example, Li^+ diffusion became faster relative to anion diffusion after introducing an ether group into the imidazolium cation in imidazolium-based ILs[10] suggesting that the chain flexibility is closely related to ion diffusion. Cheng *et al.*[31] reported 2–3 orders of anisotropy in ion conduction with respect to crystal orientation and values for D_{Li} were observed to always be smaller than the other D values at elevated temperatures on the surfaces of the crystallized polymer electrolyte. These observations also indicate that both the interactions among the mobile ions and the interactions of each ion with the cluster surfaces must be considered for understanding the migration of mobile ions in these mixtures. Interestingly, the D values obtained at x = 0.6 showed that D_{Li} and $D_{[MPEGP]}$ are similar and slowest among all the ions at both temperatures of 293 and 353 K. The ratio of $[MPEGP]^-/Li^+ \approx 2.8$ (Figure S6) was also found very close to that of $[MPEGP]^-/Li^+ \approx 3$ at x = 0.3 which showed complete ion dissociation ($\sigma_{mea}/\sigma_D \approx 1$ in Figure 1d, as will be discussed below). This result suggests that almost all Li^+ cations and $[MPEGP]^-$ anions strongly interact with each other in the sample of x=0.6.

In the samples with $x \ge 1$, all diffusion coefficients gradually decreased as LiTFSI content increased, probably due to the presence of excess LiTFSI (Figure 1a). According to the diffusion free-space model, ion diffusion depends on the interactions among the constituents and the available free space in the lower and higher concentration samples, respectively.[25] Therefore, the slower diffusion at higher concentration may be due to the lack of free space for the migration of ions resulting from over doping with LiTFSI. Similarly, the total number of mobile ions in the voids of structures is globally inversely proportional to the diffusion coefficients of ions, as shown in Figure 1a and 1b. However, the diffusion of ions in the samples with x = 0.4 and 0.5 at 293 K was faster than the diffusion in the liquid state ($0 \le x \le 0.3$). This result implies that the translational motion of mobile ions in the samples in the range of $0.4 \le x \le 1$ is closely related to the interactions of ions to the cluster surfaces.[32]

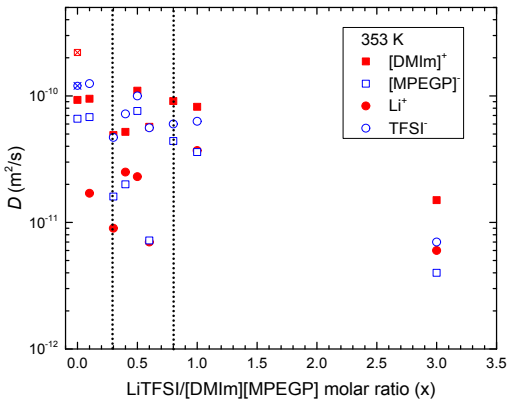

Figure 4. Variations of diffusion coefficients of $[DMIm]^+$, $[MPEGP]^-$, Li^+, and $TFSI^-$ at various relative LiTFSI contents at 353 K. Values of $D_{[DMIm]}$ (crossed square) and D_{TFSI} (crossed circle) for pure [DMIm][TFSI] were obtained from Ref. 33 and plotted at x = 0. The dotted lines are guides for the eye.

LiTFSI Dissociation (Phase I: $0 < x \le 0.3$). To gain insight into the evolution of ion–ion interactions, the ionic conductivity (σ_{mea}) was measured using impedance spectroscopy technique and compared with values calculated from ionic conductivity obtained from diffusion coefficients (σ_D) using the Nernst-Einstein formula (eq 2).

$$\sigma_D\ (\mathrm{S/cm}) = \frac{e^2}{k_B T}(n_{Li,mobile}D_{Li} + n_{TFSI,mobile}D_{TFSI} + n_{[DMIm],mobile}D_{[DMIm]} + n_{[MPEGP],mobile}D_{[MPEGP]}) \quad (2)$$

The number of ions in the unit volume of V_m ($n_{y,mobile}$) can be obtained as $(N_A \cdot x_{NMR})/V_m$, where x_{NMR} is the ion concentration determined from the NMR peak intensities (Figure 1a), y can be Li^+, $TFSI^-$, $[DMIm]^+$, or $[MPEGP]^-$, N_A is Avogadro`s number, and V_m is the molar volume of ions. In principle, $\sigma_D \geq \sigma_{mea}$ in all cases due to the assumption of complete (100%) ion dissociation in the calculation of σ_D. Therefore, the ratio of σ_{mea}/σ_D (= α) can be used to estimate the degree of ion dissociation and α = 1 corresponds to complete ion dissociation. For this calculation, it was assumed that $D_{Li} = 1 \times 10^{-16}$ m² s⁻¹ at x = 0.8 using the data obtained from the solid-state Li electrolyte at ~200 K,[24] which showed a similar ^{7}Li NMR line shape as the sample of x = 0.8.

Unexpectedly, the value of σ_{mea} (Figure 1c) when x = 0.8, which is thought to be the condition for maximum structure formation, exhibited the largest value among the measured samples including neat IL. The value of α = 0.58 for pure [DMIm][MPEGP] is in good agreement with α = 0.5 - 0.8 which was obtained from the ionic liquids composed of one type of cation and anion. Usually, LiTFSI dissolved in organic solvents, ionic liquids, or poly(ethylene oxide) provide α ≤ 0.5,[34,35] 0.5 ≤ α ≤ 0.8,[21,33] or α ≥ 0.8,[27] respectively. The electrolytes composed of poly(ethylene glycol) dimethacrylate/$LiBF_6$[26] and glyme/LiTFSI[36] also showed varied α values as a function of LiTFSI content with the maxima at O^-/Li^+ ratios of 4 - 5. This is because there is sufficient number of oxygens for complete dissociation of Li^+ cations which exists as a Li cluster of $[Li(TFSI)_{m+1}]^{m-}$ with a maximum value of m+1 = 4.[21] Similarly, the α value in these mixtures, as shown in Figure 1d, varied with LiTFSI content with a maximum value of α ≈ 1 at x = 0.3 in which the number ratio of mobile ions ($O_{[MPEGP]}^-/Li^+$) ≈ 3. The diffusion ratio of $D_{Li}/D_{[MPEGP]} \approx 1$ at x = 0.3 (see Figure 1b) also strongly suggests that all $[MPEGP]^-$ anions are bound to dissolved Li^+ cations within a Li^+–$[MPEGP]^-$ cluster. Therefore, it could be concluded that the LiTFSI cluster, $[Li(TFSI)_{m+1}]^{m-}$ with the maximum value of m+1 = 4, changed to $[Li[MPEGP]_3(TFSI)_1]^{3-}$ as shown by DFT calculations[21] (Figure S5 in Supporting Information). Moreover, the $[Li[MPEGP]_3(TFSI)_1]^{3-}$ cluster formation is in agreement with the trend of the variation of oxygen coordination number due to the presence of multiple oxygen sources in the mixtures.[15,37] For example, the numbers of oxygen atoms surrounding a Li^+ cation are ~2.5 and ~1.8 from the fluorosulfonimide anion and the polymer plasticizer, respectively, when a polymer plasticizer is added to a fluorosulfonimide-based polyether ionic melt.[37] The ternary mixed polymer electrolyte of low molecular weight poly(ethylene oxide) (PEO), LiTFSI, and *N*-methyl-*N*-propylpyrrolidinium bis(trifluoromethanesulfonyl)imide ($[PYR_{13}][TFSI]$) also showed the oxygen coordination number as 4 ~ 5 using a PEO molecule containing 2 ~ 3 oxygen atoms indicating that two PEO molecules are involved in the formation of clusters.[15]

Structure Formation and Ion Association in Clusters (Phase II: 0.3 < x ≤ 1). As LiTFSI content in the mixture is increased further beyond x = 0.3, the number of mobile Li^+ cations abruptly reduced for the cluster formation. This observation suggests that the clusters contain more Li^+ cations within a unit cluster relative to the Li^+-solvation cluster of $[Li[MPEGP]_3(TFSI)_1]^{3-}$ at x = 0.3. The relative numbers of $[MPEGP]^-$ and $TFSI^-$ anions to Li^+ cations among mobile ions became larger at x = 0.4 and 0.5 than those at x = 0.3 (Figure S6). This may be the reason for the enhancement of ion association between Li^+ cations and anions ($TFSI^-$ and $[MPEGP]^-$) similar to other ionic liquids mixed with LiTFSI.[21] When $[MPEGP]^-$ and $TFSI^-$ anions are both present, they compete with each other to interact with $[DMIm]^+$ cations due to the lack of available Li^+ cations. This complicated ion–ion interaction results in the additional peaks in the ^{31}P NMR spectra (Figure 2a). By increasing the amount of LiTFSI beyond x = 0.5, the number of mobile Li^+ cations and $[MPEGP]^-$ anions (Figure 2a) and the relative numbers of mobile $[MPEGP]^-$ anions to Li^+ cations (Figure S6) decreased up to x = 0.8. These results show that further addition of LiTFSI gradually enhances the structure formation. Moreover, in the case of x = 1.0, the number of mobile Li^+ cations and $[MPEGP]^-$ anions again increased. Thus, it can be concluded that maximum cluster formation occurs at x ≈ 0.8. From the estimated number of immobile ions at x = 0.8 (Figure 1a), it was found that the smectic structure was formed with a ratio of Li^+ : $[MPEGP]^-$: $TFSI^-$ = 1 : 1.26 : 0.32 ≈ 3:4:1 ($[Li[MPEGP]_{1.26}TFSI_{0.32}]^{0.58-}$). Therefore, it suggests that the smectic IL crystal structure possesses a negative charge: $[Li[MPEGP]_{1.26}TFSI_{0.32}]^{0.58-}$ due to an overall asymmetry with an excess of $[MPEGP]^-$ and $TFSI^-$ anions in the structures, similar to the observation from PEO-LiTFSI polymer solid electrolyte. [38,39]

This structure can easily be extended to 2-dimensional structures with each Li^+ cation surrounded by eight oxygen atoms from $[MPEGP]^-$ and $TFSI^-$ anions. Within the structures it is possible that two oxygen atoms of $TFSI^-$ can coordinate to each Li^+ cation.[40] This is in good agreement with the previous report that the smectic structure formation is mainly due to the Coulombic interaction of Li^+ cations to the phosphite head group of $[MPEGP]^-$ anions with a certain stoichiometry and the thickness of this layer is estimated as 4.36 nm.[11] In the mixtures with x > 0.8, the number of both mobile Li^+ cations and $TFSI^-$ anions increased as shown in Figure 1a, due to the lack of available $[MPEGP]^-$ anions, resulting in $[Li(TFSI)_{m+1}]^{m-}$ clusters similar to those in mixtures of IL containing $TFSI^-$ anion and LiTFSI (*vide infra*).[21]

Ion–Ion Interactions between Mobile Ions. The relative diffusion coefficients (Table 1) between ions were compared to estimate the interaction between mobile ions. Based upon the Stokes-Einstein relation for the diffusion, the variation of ion–ion interaction can be estimated from the diffusion ratio.[41] Using the model suggested by Saito *et al.*,[41] the dissociation of LiTFSI and [DMIm][MPEGP] (eqs 3 and 4) and observed diffusion coefficients (eqs 5–8) can be written as:

$$LiTFSI \rightleftharpoons Li^+ + TFSI^- \quad (3)$$

$$[DMIm][MPEGP] \rightleftharpoons [DMIm]^+ + [MPEGP]^- \quad (4)$$

$$D_{Li} = x_1 D^*_{Li} + (1 - x_1) D^*_{LiTFSI} \quad (5)$$

$$D_{TFSI} = x_1 D^*_{TFSI} + (1 - x_1) D^*_{LiTFSI} \quad (6)$$

$$D_{[DMIm]} = x_2 D^*_{[DMIm]} + (1 - x_2) D^*_{[DMIm][MPEGP]} \quad (7)$$

$$D_{[MPEGP]} = x_2 D^*_{[MPEGP]} + (1 - x_2) D^*_{[DMIm][MPEGP]} \quad (8)$$

where D^* is the inherent diffusion coefficient of each component. The relative diffusion coefficients will be:

$$D_{Li}/D_{TFSI} = D^*_{Li}/D^*_{TFSI} (x_1 \approx 1) \text{ or } 1 (x_1 \approx 0) \quad (9)$$

$$D_{[DMIm]}/D_{[MPEGP]} = D^*_{[DMIm]}/D^*_{[MPEGP]} (x_2 \approx 1) \text{ or } 1 (x_2 \approx 0) \quad (10)$$

In the same way, the association strengths between $[DMIm]^+$ and $TFSI^-$ ions and between Li^+ and $[MPEGP]^-$ ions can be estimated using the relative diffusion coefficients of $D_{[DMIm]}/D_{TFSI}$ and $D_{Li}/D_{[MPEGP]}$, respectively. The relative diffusion coefficients are close to unity when the association is quite strong between the two associated species (x_1 and $x_2 \approx 0$ in eqs 5–8). The relative diffusion coefficient $D_{[DMIm]}/D_{[MPEGP]}$ depends on the dissociation properties of LiTFSI, and therefore this ratio is not necessarily unity.[42] To estimate the strength of the interactions among the mobile ions, the relative diffusion coefficients between cations and anions (D_{cation}/D_{anion}, where cation = Li^+ or $[DMIm]^+$ and anion = $[MPEGP]^-$ or $TFSI^-$) were calculated using the D values determined at 353 K rather than at 293 K to avoid the cluster effect, which is stronger at lower temperatures. Usually LiTFSI exists as a Li cluster of $[Li(TFSI)_{m+1}]^{m-}$ in which the maximum value of m in the mixture is 4.[21] The increased ratios of $D_{Li}/D_{[MPEGP]}$ and D_{Li}/D_{TFSI} indicate enhanced LiTFSI dissociation, resulting in smaller $[Li(TFSI)_{m+1}]^{m-}$ clusters. Therefore, the increases of $D_{Li}/D_{[MPEGP]}$ and D_{Li}/D_{TFSI} up to x = 0.4 reveal gradual increases of Li^+ cation dissociation (Table 1). Similar behavior was observed in the LiTFSI dissolved ionic liquids, 1-butyl-3-methylimidazolium bis(trifluoromethanesulfonyl)imide ([BMIm]TFSI) and 1-butyl-2,3-dimethylimidazolium bis(trifluoromethanesulfonyl)imide ([BDMIm]TFSI): the ratio of D_{Li}/D_{TFSI} increases when increasing the content of LiTFSI up to 24 wt %.[41]

After the structure formation at $0.4 \leq x$ (Figure S1), the diffusion ratios changed in a complicated manner, probably because of the variations of the number of mobile ions for each ion type. In the range of $0.4 \leq x \leq 0.8$, the ratios of D_{Li}/D_{TFSI} and $D_{Li}/D_{[MPEGP]}$ tend to decrease with the minimum at x = 0.8, as predicted from the line broadening of ^{7}Li NMR spectra. The slower diffusion of mobile Li^+ cations compared to the other ions in this range may be the result of the interactions of Li^+ cations with the negatively charged clusters ($[Li[MPEGP]_{1.26}(TFSI)_{0.32}]^{0.58-}$), similar to observations from LiTFSI doped polymer electrolytes that have negatively charged chains.[12,13,26,41] The x = 0.8 sample also revealed $D_{[DMIm]}/D_{TFSI} = 1.52$, which is close to the value of 1.83 for the bulk [DMim][MPEGP] (x = 0). This result indicates that the unavailability of Li^+ cations and $[MPEGP]^-$ anions enhances the ion–ion interaction between $[DMIm]^+$ cations and $TFSI^-$ anions.

In the samples with x > 0.8, which have LiTFSI concentrations more than enough to consume $[MPEGP]^-$ anions for clustering, the ratios of D_{Li}/D_{TFSI}, $D_{Li}/D_{[MPEGP]}$, and $D_{[DMIm]}/D_{TFSI}$ are the largest in the x = 3 sample. Notably, D_{Li}/D_{TFSI} (=0.86) and $D_{[DMIm]}/D_{TFSI}$ (= 2.14) from the x = 3 sample are similar to those of LiTFSI saturated pyrrolidinium-based ionic liquid ($D_{Li}/D_{TFSI} = 0.81$)[21] and of neat [DMIm][TFSI] material ($D_{[DMIm]}/D_{TFSI}$ = 1.83),[33] respectively. These observations indicate that the ion–ion interactions among the constituent ions are similar again to those in the bulk ionic liquid at x = 3, which has the LiTFSI exceeding the proper amounts for consumption of all $[MPEGP]^-$ anions.

Table 1. Relative Diffusion Coefficients of LiTFSI and [DMIm][MPEGP] Mixtures as a Function of LiTFSI Content (x) at 353 K.

x	$D_{[DMIm]}/D_{TFSI}$	D_{Li}/D_{TFSI}	$D_{Li}/D_{[MPEGP]}$
0	1.83[a]	–	–
0.1	0.76	0.14	0.25
0.3	1.04	0.19	0.56
0.4	0.72	0.35	1.25
0.5	1.1	0.23	0.30
0.6	1.02	0.13	0.97
0.8	1.52	N/A	N/A
1	1.30	0.59	1.03
3	2.14	0.86	1.5

[a] $D_{[DMIm]}/D_{TFSI}$ for pure [DMIm][TFSI] was calculated using diffusion coefficient values reported in literature.[33]

Li$^+$ Cation Transference Number. The Li^+ cation transference number (t_{Li}) represents the contribution of Li^+ cations in the overall ionic conductivity of the electrolyte and it is directly related to the performance of Li-ion batteries. It can be calculated from diffusion coefficients using the formula:

$t_{Li,mobile}$ =

$$\frac{n_{\mathrm{Li,mobile}}D_{\mathrm{Li}}}{n_{\mathrm{Li,mobile}}D_{\mathrm{Li}}+n_{\mathrm{TFSI,mbile}}D_{\mathrm{TFSI}}+n_{\mathrm{[DMIm],mobile}}D_{\mathrm{[DMIm],mobile}}+n_{\mathrm{[MPEGP],mobile}}D_{\mathrm{[MPEGP]}}} \quad (11)$$

where $n_{y,mobile}$ and D_y are the number of mobile ions in molar concentration and diffusion coefficients, respectively, for y = Li^+, $TFSI^-$, $[DMIm]^+$, and [MPEGP]. Here, the molar concentrations (numbers) of mobile ions ($n_{y,mobile}$) estimated from the peak intensities (Figure 1a) were used to calculate the $t_{Li,mobile}$ value for mobile ions. Usually, the lithium transference number is proportional to the Li salt concentration in the bulk liquids[21,30] as observed from the $t_{Li,x}$, which was calculated using nominal LiTFSI concentration, x. However, the $t_{Li,mobile}$ calculated from the number of mobile ions using the diffusion coefficients determined at 353 K (represented in Figure 5) decreased with an increase of LiTFSI in the range of $0.5 \le x \le 0.8$. While the D_{Li} value for x = 0.8 is not available, this sample is expected to give the smallest $t_{Li,mobile}$ value due to small values of $n_{Li,mobile}$ and D_{Li} for mobile Li^+ cations. The value of $t_{Li,mobile}$ is also smaller than $t_{Li,x}$, calculated using the nominal concentration of ions. It is worth mentioning that the number of mobile ions should be considered for the calculation of Li^+ cation transference number in the polymerized electrolytes as well because it is easy to neglect the fact that the number of mobile ions is smaller than the nominal concentration due to the interactions between ions and the clusters.

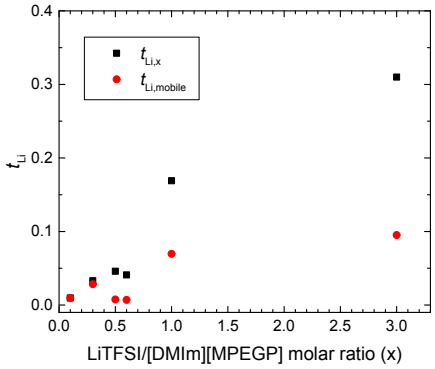

Figure 5. Values of Li transference number (t_{Li}) for LiTFSI and [DMIm][MPEGP] mixtures as a function of LiTFSI content at 353 K. Values of $t_{Li,mobile}$ were calculated using the ion concentrations determined using NMR peak intensities (Figure 1a) while the nominal content of x was used to calculate $t_{Li,x}$ values.

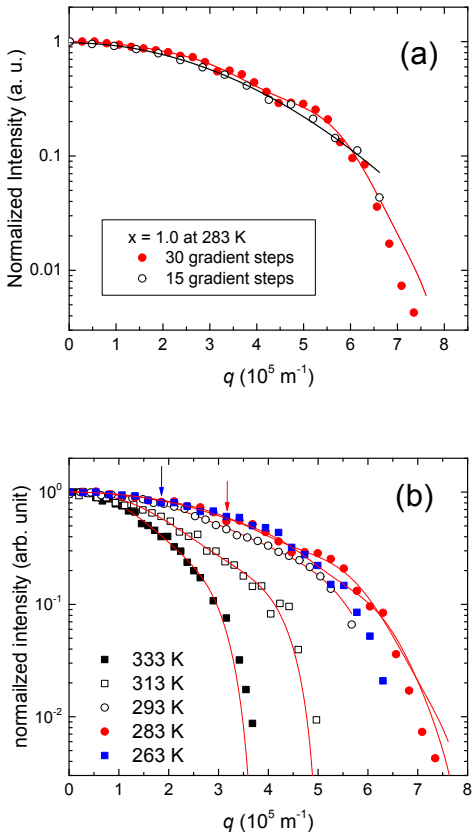

Figure 6. (a) ^{7}Li PFG echo profiles of x = 1.0 mixture sample obtained using 15 and 30 gradient steps from 4.7 to ~ 2000 G/cm with Δ = 50 ms and δ = 2 ms and fitted with the Stejskal-Tanner formula (eq 1) and NMR-diffraction equation (eq 12), respectively. (b) ^{7}Li PFG echo profiles of x = 1.0 sample obtained at various temperatures with Δ = 50 ms. Solid lines are fitting curves using eq 1. The blue and red arrows at q = 1.85 × 10^5 and 3.16 ×10^5 m^{-1} indicate the first echo minima at 263 and 283 K, respectively.

Size of Ionic Liquid Crystals: NMR Diffraction. The ^{7}Li PFG-echo profile obtained with 15 gradient steps for x = 1.0 sample is represented in Figure 6a. These data are fit well with the Stejskal-Tanner equation even though a little scattering is observed on the decay. However, the echo obtained with 30 gradient steps showed a clear minimum, or so-called 'NMR diffraction'. Usually, the NMR diffraction pattern on a PFG-echo profile appears due to a diffusion barrier existing in the sample.[12,13,41,43] Thus, we confirmed the structure formed from the interactions between the Li^+ cation and $[MPEGP]^-$ anion performing as a diffusion barrier. The first minimum on the PFG-NMR echo profile at q (= $(2\pi)^{-1}(\gamma g\delta)$) is related to the size of the cluster: $q = b^{-1}$, where q is the area of gradient strength and b is the distance between the pores.[43] The echo decay with NMR-diffraction curve can be fitted using eq 12.[43]

$$E(q,\Delta) = |s_0(q)|^2 \exp\left[-\frac{6D_{eff}\Delta}{b^2+3\xi^2}\left(1-\exp(-2\pi^2q^2\xi^2)\frac{\sin(2\pi qb)}{2\pi qb}\right)\right] \quad (12)$$

where the local structure factor of S_o is

$$s_0(q) = \frac{\sin(\pi qa)}{\pi qa} \quad (13)$$

and ξ is the standard deviation of the mean pore distance of b, a is the pore size, D_{eff} is the diffusion coefficient for migration between the pores, and Δ is the diffusion time. Therefore, in this study, b and a correspond to the cluster size and the distance between the clusters (pore size), respectively, and D_{eff} is the diffusion coefficient of ions in the vicinity of the cluster surfaces. The cluster size, which corresponds to the pore distance b in eq. 12, can be directly estimated from the first echo minima using the relationship of $q = b^{-1}$.[43,44] In Figure 6b, the first echo minima from ^{7}Li PFG-NMR of x = 1.0 give the estimated cluster size of $b = q^{-1} = 5.4$ and 3.2 μm, which are in reasonable agreement with b = 4.4 and 3.2 μm from the curve fitting to eq 12 (Table S1) at 263 and 283 K, respectively. At higher temperatures, it was impossible to measure the cluster size directly from the first echo minima due to its ambiguity. This may be a consequence of the structural heterogeneity induced by chain flexibility at high temperatures. At lower temperatures, the structure formation and the interactions of Li^+ cations with the cluster surfaces are enhanced, as revealed by the larger value of D after gelation (Figures 1b, and 4) and the broader line width of ^{7}Li NMR spectra (Figure S7).

The measured cluster sizes (Table S1) showed that it gradually increased with a decrease of temperature similar to the lithium polymer electrolytes containing glucitol.[14] The pore sizes (a) of 0.75 and 0.5 μm, obtained from ^{1}H PFG echo profiles of the x = 1.0 sample (Figure S8) for the $[DMIm]^+$ cation and $[MPEGP]^-$ anion, respectively, are smaller by about one-half compared to a = 1.2 μm obtained from ^{7}Li PFG-NMR (Table S1). This difference between ^{7}Li and ^{1}H/^{19}F PFG echo profiles for determining the pore size was observed in previous research,[12,14] which revealed that the weak amplitude of echo minima in ^{1}H PFG echo profiles gives a smaller a as predicted by Eqs 12 and 13. In this study, the ^{1}H PFG-echo profiles (Figure S8) also showed a weaker NMR diffraction than ^{7}Li PFG-echo profiles. Therefore, the smaller values for a are a consequence of the weak amplitude of the first echo minima. The amplitude differences are most likely a result of the distances between each of the ions and the cluster surface because of their charge differences. Based on our observations (*vide supra*), an average cluster is negatively charged ($[Li[MPEGP]_{1.26}TFSI_{0.32}]^{0.58-}$). Therefore, the distance between mobile ions and the cluster surface may increase in the order of Li^+ < $[DMIm]^+$ < $[MPEGP]^-$ owing to their electrostatic interactions. Consequently, the diffraction observed in the ^{7}Li PFG-echo profile is the strongest, and in the ^{1}H PFG-echo profile it is weaker from $[MPEGP]^-$ anions than from $[DMIm]^+$ cations (Figure S8). For this reason, ^{7}Li PFG echo profiles were used to determine the cluster size of the structure (Figure 7a). The cluster size, which is smaller than the pore size, steeply increased at 0.4 ≤ x ≤ 1 and the differences became smaller when the cluster size increased (up to x = 1). Meanwhile, the cluster and pore sizes at x = 3 appeared slightly smaller than those obtained at x = 1. This may be due to an error in the fitting because of weak diffraction behavior (Figure S9). Even though the echo profile is obviously closer to the NMR-diffraction pattern than the bulk diffusion at x = 3 (Figure S9), it is not well fitted with either the Stejskal-Tanner formula (eq 1) or the diffraction equation (eq 12). This unclear diffraction may be due to the presence of excess LiTFSI. The relative diffusion coefficients, D_{Li}/D_{TFSI} and $D_{[DMIm]}/D_{TFSI}$ (Table 1), indicate that the mobile Li^+ cations behave like those in the bulk liquid for the x = 3 sample. In this situation, the ^{7}Li PFG-echo profiles are obtained mainly from the bulk-like Li^+ cations, which diffuse through the center of voids (far away from the cluster surfaces) and they may not be sensitive to the structure of the clusters. This may cause smaller values of a and b as we discussed above by comparing ^{7}Li and ^{1}H PFG-echo profiles (Figure S8). From the NMR diffraction, it was found that the cluster size is inversely proportional to the number of mobile $[MPEGP]^-$ anions. Based on the above observations, it may be concluded that the cluster size (b) at x = 3 would be 1.7 μm (*i.e*, similar to that obtained from the x = 1 sample).

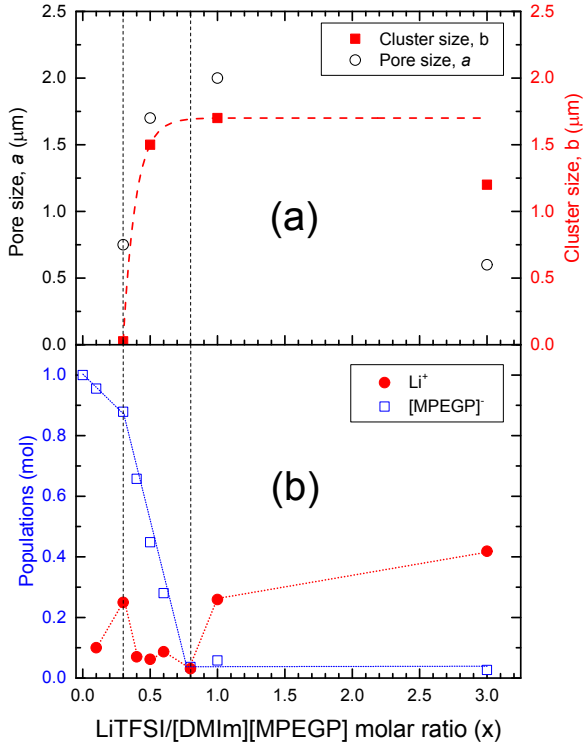

Figure 7. (a) Cluster size, b and pore size, a obtained from ^{7}Li PFG echo profiles at 313 K. (b) Mobile ion populations calculated from intensities of ^{7}Li and ^{31}P NMR spectra (Figure 2) in the mixtures of LiTFSI and [DMIm][MPEGP] as a function of LiTFSI content. Dashed lines are guides for the eye.

From the NMR diffraction behavior (eq 12), it is possible to determine the diffusion coefficient of ions migrating between the pores (*i.e.*, on the cluster surfaces), the so-called 'effective diffusion coefficient (D_{eff}). Usually, D_{eff} and the bulk diffusion coefficient (D) are identical when there are negligible interactions between the migrating ions and the cluster surfaces.[43] Surprisingly, after the mixtures of LiTFSI and [DMIm][MPEGP] form visible structures ($x \geq 0.4$) D_{eff} is three orders of magnitude faster than D, which is a steady-state diffusion coefficient obtained using the Stejskal-Tanner equation without considerations of the oscillatory motion of the echo profiles (Table S1 and Figure S10). This enhancement of D_{eff} in this system is quite interesting behavior compared with other LiTFSI doped polymer electrolytes that show a diffraction pattern on the PFG echo profiles but with similar values of D and D_{eff}.[12-14] The diffraction pattern from the ^{1}H PFG-echo profile of $[DMIm]^+$ cation at x =1 (Figure S8) also gave $D_{eff} \approx 10^{-7}$ m^2 s^{-1}. This fast D_{eff} may contribute to a higher total ionic conductivity for the mixtures in the molar ratio range of $0.4 \leq x \leq 1$ compared to other samples including the neat ionic liquid.

CONCLUSIONS

The sizes of ionic liquid crystals and the contributions of each ion on the structure formation in mixtures of LiTFSI and [DMIm][MPEGP] were studied using analyses of NMR diffraction and intensities of ^{7}Li, ^{1}H, ^{19}F, and ^{31}P NMR peaks, respectively, as a function of LiTFSI content. The steady-state diffusion coefficients for each mobile ion were also determined using ^{7}Li, ^{1}H, and ^{19}F PFG-NMR examinations and compared with the estimated ion–ion interactions between the mobile ions. The ^{7}Li PFG-NMR echo profiles showed cluster sizes up to ~1.7 μm, which is inversely proportional to the number of mobile $[MPEGP]^-$ anions. The steady-state diffusion coefficients for mobile ions are comparable with the value of D for neat [DMIm][MPEGP]. The relative diffusion coefficients between cations and anions varied with LiTFSI concentration and reached values comparable to those of to the neat ionic liquid values in the mixture with x = 3. The lithium transference number was reduced tremendously in the range $0.4 \leq x \leq 0.8$ due to the reduced number of mobile Li^+ cations and decreased D_{Li}. At x = 0.3, the relations of $\sigma_{mea}/\sigma_D \approx 1$ and $D_{Li}/D_{[MPEGP]} \approx 1$ reflect the fact that the $[LiTFSI_{m+1}]^{m-}$ clusters are completely dissociated by solvent and $[MPEGP]^-$ anions have a solvation structure of $[Li(MPEGP)_3(TFSI)_1]^{3-}$,which is estimated based on the ratio of $O_{[MPEGP]^-}/Li^+ \approx 3$. The numbers of immobile ions estimated at x = 0.8, with maximum structure formation, indicated that the structure is composed of $[Li(MPEGP)_{1.26}(TFSI)_{0.32}]^{0.58-}$ (Li^+ : $[MPEGP]^-$: $TFSI^- \approx 3 : 4 : 1$). This is in very good agreement with the number of oxygen atoms that can be coordinated with Li^+ cations by the Coulombic interaction. In summary, the mixtures can be discriminated and categorized into three distinct states of so-called local interaction ($x \leq 0.3$), global structure formation ($0.4 \leq x \leq 1$), and LiTFSI excess ($x < 1$) states. The Coulombic interactions between Li^+ cations and $[MPEGP]^-$ anions were found as the main reason for the formation of structure with an accurate stoichiometry.

ASSOCIATED CONTENT

Supporting Information

The Supporting Information is available free of charge on the ACS Publications website at DOI:
A photo of samples, SAXS data, illustrated phase structures, DFT results, and NMR diffraction data are available.

AUTHOR INFORMATION

Corresponding Authors

*E-mail: leejs70@khu.ac.kr.
*E-mail: karl.mueller@pnnl.gov.

ORCID

Kee Sung Han: 0000-0002-3535-1818
Je Seung Lee: 0000-0002-5033-7109
Vijayakumar Murugesan: 0000-0001-6149-1702
Karl T. Mueller: 0000-0001-9609-9516

Author Contributions

‡S. K. Park and ‡K. S. Han contributed equally to this work.

Notes

The authors declare no competing financial interests.

ACKNOWLEDGMENT

This work was financially supported by a grant from the Fundamental R&D Program for Core Technology of Materials, and Industrial Strategic Technology Development Program funded by the Ministry of Knowledge Economy, Republic of Korea, and partially supported by Materials Architecturing Research Center of Korea Institute of Science and Technology (KIST). This research was also supported by Basic Science Research Program through the National Research Foundation of Korea (NRF) funded by the Ministry of Education (2018R1D1A1B07050522). Synchrotron X-ray diffraction examinations were performed at Pohang Light Source, South Korea, and NMR experiments were performed at EMSL, a DOE Office of Science user facility sponsored by the DOE BER located at PNNL.

REFERENCES

(1) Olivier-Bourbigou, H.; Magna, L.; Morvan, D. Ionic liquids and catalysis: Recent progress from knowledge to applications. *Appl. Catal. A: Gen.* **2010**, *373*, 1-56.

(2) Zhang, S.; Sun, N.; He, X.; Lu, X.; Zhang, X. Physical Properties of Ionic Liquids: Database and Evaluation. *J. Phys. Chem. Ref. Data* **2006**, *35*, 1475-1517.

(3) Li, S.; Han, K. S.; Feng, G.; Hagaman, E. W.; Vlcek, L.; Cummings, P. T. Dynamic and Structural Properties of Room-Temperature Ionic Liquids near Silica and Carbon Surfaces. *Langmuir* **2013**, *29*, 9744-9749.

(4) Han, K. S.; Wang, X.; Dai, S.; Hagaman, E. W. Distribution of 1-Butyl-3-methylimidazolium Bistrifluoromethylsulfonimide in Mesoporous Silica As a Function of Pore Filling. *J. Phys. Chem. C* **2013**, *117*, 15754-15762.

(5) Le Bideau, J.; Viau, L.; Vioux, A. Ionogels, ionic liquid based hybrid materials. *Chem. Soc. Rev.* **2011**, *40*, 907-925.

(6) Armand, M.; Endres, F.; MacFarlane, D. R.; Ohno, H.; Scrosati, B. Ionic-liquid materials for the electrochemical challenges of the future. *Nat. Mater.* **2009**, *8*, 621-629.

(7) Lu, Y.; Korf, K.; Kambe, Y.; Tu, Z.; Archer, L. A. Ionic-Liquid–Nanoparticle Hybrid Electrolytes: Applications in Lithium Metal Batteries. *Angew. Chem. Int. Ed.* **2014**, *53*, 488-492.

(8) Liao, C.; Sun, X.-G.; Dai, S. Crosslinked gel polymer electrolytes based on polyethylene glycol methacrylate and ionic liquid for lithium ion battery applications. *Electrochim. Acta* **2013**, *87*, 889-894.

(9) Appetecchi, G. B.; Kim, G. T.; Montanino, M.; Alessandrini, F.; Passerini, S. Room temperature lithium polymer batteries based on ionic liquids. *J. Power Sources* **2011**, *196*, 6703-6709.

(10) Liao, C.; Shao, N.; Han, K. S.; Sun, X.-G.; Jiang, D.-E.; Hagaman, E. W.; Dai, S. Physicochemical properties of imidazolium-derived ionic liquids with different C-2 substitutions. *Phys. Chem. Chem. Phys.* **2011**, *13*, 21503-21510.

(11) Lee, J. H.; Han, K. S.; Lee, J. S.; Lee, A. S.; Park, S. K.; Hong, S. Y.; Lee, J.-C.; Mueller, K. T.; Hong, S. M.; Koo, C. M. Facilitated Ion Transport in Smectic Ordered Ionic Liquid Crystals. *Adv. Mater.* **2016**, *28*, 9301-9307.

(12) Hayamizu, K.; Akiba, E.; Price, W. S. Ion Diffusion Restricted by Time-Dependent Barriers in a Viscous Polyethylene-Based Liquid Electrolyte. *Macromolecules* **2003**, *36*, 8596-8598.

(13) Hayamizu, K.; Akiba, E.; Bando, T.; Aihara, Y.; Price, W. S. NMR Studies on Poly(ethylene oxide)-based Polymer Electrolytes with Different Cross-Linking Doped with $LiN(SO_2CF_3)_2$. Restricted Diffusion of the Polymer and Lithium Ion and Time-Dependent Diffusion of the Anion. *Macromolecules* **2003**, *36*, 2785-2792.

(14) Saito, Y.; Hirai, K.; Katayama, H.; Abe, T.; Yokoe, M.; Aoi, K.; Okada, M. Ionic Diffusion Mechanism of Glucitol-Containing Lithium Polymer Electrolytes. *Macromolecules* **2005**, *38*, 6485-6491.

(15) Diddens, D.; Heuer, A. Simulation Study of the Lithium Ion Transport Mechanism in Ternary Polymer Electrolytes: The Critical Role of the Segmental Mobility. *J. Phys. Chem. B* **2014**, *118*, 1113-1125.

(16) Kunze, M.; Paillard, E.; Jeong, S.; Appetecchi, G. B.; Schönhoff, M.; Winter, M.; Passerini, S. Inhibition of Self-Aggregation in Ionic Liquid Electrolytes for High-Energy Electrochemical Devices. *J. Phys. Chem. C* **2011**, *115*, 19431-19436.

(17) Bogle, X.; Vazquez, R.; Greenbaum, S.; Cresce, A. v. W.; Xu, K. Understanding Li^+–Solvent Interaction in Nonaqueous Carbonate Electrolytes with ^{17}O NMR. *J. Phys. Chem. Lett.* **2013**, *4*, 1664-1668.

(18) Wallace, M.; Iggo, J. A.; Adams, D. J. Using solution state NMR spectroscopy to probe NMR invisible gelators. *Soft Matter* **2015**, *11*, 7739-7747.

(19) Stejskal, E. O.; Tanner, J. E. Spin Diffusion Measurements: Spin Echoes in the Presence of a Time-Dependent Field Gradient. *J. Chem. Phys.* **1965**, *42*, 288-292.

(20) Johnson Jr, C. S. Diffusion ordered nuclear magnetic resonance spectroscopy: principles and applications. *Prog. Nucl. Magn. Reson. Spectrosc.* **1999**, *34*, 203-256.

(21) Frömling, T.; Kunze, M.; Schönhoff, M.; Sundermeyer, J.; Roling, B. Enhanced Lithium Transference Numbers in Ionic Liquid Electrolytes. *J. Phys. Chem. B* **2008**, *112*, 12985-12990.

(22) Spitz, F. R.; Cabral, J.; Haake, P. Cation effects on one bond phosphorus-hydrogen coupling constants in phosphinate ion (hypophosphite ion). Experimental evidence for the effect of association with metal cations on the structure of tetracoordinate phosphorus anions in solution. *J. Am. Chem. Soc.* **1986**, *108*, 2802-2805.

(23) Gupta, A.; Murugan, R.; Paranthaman, M. P.; Bi, Z.; Bridges, C. A.; Nakanishi, M.; Sokolov, A. P.; Han, K. S.; Hagaman, E. W.; Xie, H.; Mullins, C. B.; Goodenough, J. B. Optimum lithium-ion conductivity in cubic $Li_{7-x}La_3Hf_{2-x}Ta_xO_{12}$. *J. Power Sources* **2012**, *209*, 184-188.

(24) Buschmann, H.; Dolle, J.; Berendts, S.; Kuhn, A.; Bottke, P.; Wilkening, M.; Heitjans, P.; Senyshyn, A.; Ehrenberg, H.; Lotnyk, A.; Duppel, V.; Kienle, L.; Janek, J. Structure and dynamics of the fast lithium ion conductor "$Li_7La_3Zr_2O_{12}$". *Phys. Chem. Chem. Phys.* **2011**, *13*, 19378-19392.

(25) Pickup, S.; Blum, F. D. Self-diffusion of toluene in polystyrene solutions. *Macromolecules* **1989**, *22*, 3961-3968.

(26) Kataoka, H.; Saito, Y.; Uetani, Y.; Murata, S.; Kii, K. Interactive Effect of the Polymer on Carrier Migration Nature in the Chemically Cross-Linked Polymer Gel Electrolyte Composed of Poly(ethylene glycol) Dimethacrylate. *J. Phys. Chem. B* **2002**, *106*, 12084-12087.

(27) Hayamizu, K.; Sugimoto, K.; Akiba, E.; Aihara, Y.; Bando, T.; Price, W. S. An NMR and Ionic Conductivity Study of Ion Dynamics in Liquid Poly(ethylene oxide)-Based Electrolytes Doped with $LiN(SO_2CF_3)_2$. *J. Phys. Chem. B* **2001**, *106*, 547-554.

(28) Pregosin, P. S.; Kumar, P. G. A.; Fernández, I. Pulsed Gradient Spin–Echo (PGSE) Diffusion and $^1H,^{19}F$ Heteronuclear Overhauser Spectroscopy (HOESY) NMR Methods in Inorganic and Organometallic Chemistry: Something Old and Something New. *Chem. Rev.* **2005**, *105*, 2977-2998.

(29) Nicotera, I.; Oliviero, C.; Henderson, W. A.; Appetecchi, G. B.; Passerini, S. NMR Investigation of Ionic Liquid–LiX Mixtures: Pyrrolidinium Cations and TFSI- Anions. *J. Phys. Chem. B* **2005**, *109*, 22814-22819.

(30) Hayamizu, K.; Aihara, Y.; Nakagawa, H.; Nukuda, T.; Price, W. S. Ionic Conduction and Ion Diffusion in Binary Room-Temperature Ionic Liquids Composed of [emim][BF_4] and $LiBF_4$. *J. Phys. Chem. B* **2004**, *108*, 19527-19532.

(31) Cheng, S.; Smith, D. M.; Li, C. Y. How Does Nanoscale Crystalline Structure Affect Ion Transport in Solid Polymer Electrolytes? *Macromolecules* **2014**, *47*, 3978-3986.

(32) Every, H. A.; Bishop, A. G.; MacFarlane, D. R.; Oradd, G.; Forsyth, M. Room temperature fast-ion conduction in imidazolium halide salts. *J. Mater. Chem.* **2001**, *11*, 3031-3036.

(33) Tokuda, H.; Hayamizu, K.; Ishii, K.; Susan, M. A. B. H.; Watanabe, M. Physicochemical Properties and Structures of Room Temperature Ionic Liquids. 2. Variation of Alkyl Chain

Length in Imidazolium Cation. *J. Phys. Chem. B* **2005**, *109*, 6103-6110.

(34) Hayamizu, K.; Aihara, Y.; Arai, S.; Garcia. Pulse-Gradient Spin-Echo ^{1}H, ^{7}Li, and ^{19}F NMR Diffusion and Ionic Conductivity Measurements of 14 Organic Electrolytes Containing $LiN(SO_2CF_3)_2$. *J. Phys. Chem. B* **1999**, *103*, 519-524.

(35) Tokuda, H.; Tabata, S.-i.; Susan, M. A. B. H.; Hayamizu, K.; Watanabe, M. Design of Polymer Electrolytes Based on a Lithium Salt of a Weakly Coordinating Anion to Realize High Ionic Conductivity with Fast Charge-Transfer Reaction. *J. Phys. Chem. B* **2004**, *108*, 11995-12002.

(36) Zhang, C.; Ueno, K.; Yamazaki, A.; Yoshida, K.; Moon, H.; Mandai, T.; Umebayashi, Y.; Dokko, K.; Watanabe, M. Chelate Effects in Glyme/Lithium Bis(trifluoromethanesulfonyl)amide Solvate Ionic Liquids. I. Stability of Solvate Cations and Correlation with Electrolyte Properties. *J. Phys. Chem. B* **2014**, *118*, 5144-5153.

(37) Geiculescu, O. E.; Hallac, B. B.; Rajagopal, R. V.; Creager, S. E.; DesMarteau, D. D.; Borodin, O.; Smith, G. D. The Effect of Low-Molecular-Weight Poly(ethylene glycol) (PEG) Plasticizers on the Transport Properties of Lithium Fluorosulfonimide Ionic Melt Electrolytes. *J. Phys. Chem. B* **2014**, *118*, 5135-5143.

(38) Molinari, N.; Mailoa, J. P.; Kozinsky, B. Effect of Salt Concentration on Ion Clustering and Transport in Polymer Solid Electrolytes: A Molecular Dynamics Study of PEO–LiTFSI. *Chem. Mater.* **2018**, *30*, 6298-6306.

(39) Pesko, D. M.; Timachova, K.; Bhattacharya, R.; Smith, M. C.; Villaluenga, I.; Newman, J.; Balsara, N. P. Negative Transference Numbers in Poly(ethylene oxide)-Based Electrolytes. *J. Electrochem. Soc.* **2017**, *164*, E3569-E3575.

(40) Umecky, T.; Saito, Y.; Okumura, Y.; Maeda, S.; Sakai, T. Ionization Condition of Lithium Ionic Liquid Electrolytes under the Solvation Effect of Liquid and Solid Solvents. *J. Phys. Chem. B* **2008**, *112*, 3357-3364.

(41) Saito, Y.; Umecky, T.; Niwa, J.; Sakai, T.; Maeda, S. Existing Condition and Migration Property of Ions in Lithium Electrolytes with Ionic Liquid Solvent. *J. Phys. Chem. B* **2007**, *111*, 11794-11802.

(42) Saito, Y.; Hirai, K.; Matsumoto, K.; Hagiwara, R.; Minamizaki, Y. Ionization State and Ion Migration Mechanism of Room Temperature Molten Dialkylimidazolium Fluorohydrogenates. *J. Phys. Chem. B* **2005**, *109*, 2942-2948.

(43) Callaghan, P. T.; Coy, A.; MacGowan, D.; Packer, K. J.; Zelaya, F. O. Diffraction-like effects in NMR diffusion studies of fluids in porous solids. *Nature* **1991**, *351*, 467-469.

(44) Kuntz, J.-F.; Palmas, P.; Canet, D. Diffusive diffraction measurements in porous media: Effect of structural disorder and internal magnetic field gradients. *J. Magn. Reson.* **2007**, *188*, 322-329.

Table of Contents